2014

Comparative development and evolution of two lateral line phenotypes in Lake Malawi cichlids

Jacqueline F. Webb
University of Rhode Island, jacqueline_webb@uri.edu

Nathan C. Bird

See next page for additional authors

Citation/Publisher Attribution
Webb, JF, Bird, NC, Carter, L, Dickson, J. 2014. Comparative development and evolution of two lateral line phenotypes in Lake Malawi cichlids. *Journal of Morphology.* DOI 10.1002/jmor.20247.

COMPARATIVE DEVELOPMENT AND EVOLUTION OF TWO LATERAL LINE PHENOTYPES IN LAKE MALAWI CICHLIDS

Jacqueline F. Webb*, Nathan C. Bird, Lauren Carter, and Juleen Dickson

Department of Biological Sciences, University of Rhode Island, 120 Flagg Road, Kingston, RI 02881, USA

*Corresponding author: Dr. Jacqueline F. Webb, Department of Biological Sciences, University of Rhode Island, 120 Flagg Road, Kingston, RI 02881, USA. Email: Jacqueline_webb@mail.uri.edu

Short Title: Development and Evolution of Cichlid Lateral Line

ABSTRACT A comparison of the pattern and timing of development of cranial lateral line (LL) canals and canal neuromasts in three species of Lake Malawi cichlids, *Labeotropheus fuelleborni* and *Metriaclima zebra* (narrow LL canals), and *Aulonocara baenschi* (widened LL canals) were used to test the hypothesis that the evolution of widened canals (an adaptive phenotype in the lateral line system) from narrow canals is the result of heterochrony. Using histological analysis and SEM, this study has provided the first detailed and quantitative description of the development of widened lateral line canals in a teleost, and demonstrated that: 1) canal neuromast number and the pattern of canal morphogenesis are conserved among species with different adult canal morphologies, 2) heterochrony ("dissociated heterochrony" in particular) can explain the evolution of widened canals and variation in morphology between canals in a species with respect to canal diameter and neuromast size, and 3) the morphology of the lateral line canals and the dermal bones in which they are found (e.g., the mandibular canal contained within the dentary and anguloarticular bones of the mandible) can evolve independently of each other, thus requiring the addition of another level of complexity to discussions of modularity and integration in the skull of bony fishes.

KEY WORDS: Cichlidae; neuromast; lateral line; heterochrony; modularity, dermatocranium, hair cell

INTRODUCTION

The mechanosensory lateral line system of fishes detects unidirectional and low frequency oscillatory water flows and plays critical roles in prey detection and other behaviors (reviewed in Webb, et al., 2008). Directionally sensitive neuromast receptor organs are distributed on the skin (superficial neuromasts) as well as in canals (canal neuromasts) on the head, trunk and tail. The cranial lateral line canals, which are integrated into a conserved subset of the dermatocranial elements of bony fishes, demonstrate well-defined morphological variation among bony fishes and among teleosts in particular (narrow, widened, reduced and branched canals; Webb, 1989b). Narrow canals, the most common of the four canal morphologies, are well-ossified with small pores that connect the fluid within the canal with the outside environment. In contrast, widened canals have evolved convergently in only about a dozen families of typically benthic or deep-water marine and freshwater teleosts. Widened canals are larger in diameter than narrow canals, may cover much of the head, and typically contain large neuromasts. The canal roof is weakly ossified and dominated by large bony canal pores, which are covered by an epithelium that is pierced by very small "epithelial pores" that provide the connection between the fluid within the canal and the external environment. Narrow and widened cranial lateral line canals have been shown to be functionally distinct (Webb, et al., 2008; Denton and Gray, 1988, 1989) and it has been suggested that the evolution of canal morphology among teleosts is the result of heterochrony, or evolutionary changes in developmental timing (Webb 1989a). The study of closely related species with narrow and widened canals provide an interesting context for the integrative study of the adaptive evolution of the lateral line system, but it requires detailed analyses of lateral line development.

The development of the lateral line system has been studied in detail in only a small number of species, all of which have narrow canals. It has been described as occurring in three phases [5]. Migration of neuromast primordia from the cranial lateral line placodes establishes spatial patterning of neuromasts in embryos and early larvae (as elegantly detailed in the posterior lateral line system of zebrafish, *Danio rerio*; reviewed in Nunez et al., 2009; Aman and Piotrowski, 2011; Chitnis et al., 2011). Then development continues with neuromast growth (increase in size, change in shape) revealing distinctions between presumptive canal neuromasts (those that will eventually become enclosed in canals) from other superficial neuromasts (that will remain on the skin; e.g., Webb and Shirey, 2003). Finally, in late stage larvae, morphogenesis of the lateral line canals is initiated around individual canal neuromasts to initially form tubular canal segments, a process that occurs in four stages (Webb and Shirey, 2003; Tarby and Webb, 2003): Stage I - neuromast differentiates in the epithelium, Stage II - neuromast sinks into an epithelial depression and then canal walls emerge from the dermal bone below the neuromast and ossify, Stage III - epithelium encloses the neuromast forming a canal segment, and Stage IV - ossified canal walls meet over the neuromast forming the ossified canal roof. As they are forming, canal segments are increasing in diameter (Tarby and Webb, 2003; Moore and Webb, 2008). Adjacent segments are also growing towards one another and fuse leaving a common pore between them (e.g., Allis, 1889), thus accounting for the alternating positions of neuromasts and pores along the length of the cranial canals in most bony fishes (Webb and Northcutt, 1997).

The hypothesis that heterochrony can explain phenotypic evolution in the lateral line system of bony fishes has been posed (Webb, 1989b; Webb, 1990), but not explicitly tested. The evolution of reduced and branched cranial lateral line canals from narrow canals has been

hypothesized to be the result of the simple truncation/deceleration (paedomorphic trend) or extension/acceleration (peramorphic trend) of canal morphogenesis, respectively (Webb, 1989b). In contrast, the evolution of widened canals appears to be the result of "dissociated heterochrony", defined as a mixture of the evolution of peramorphic and paedomorphic features (McNamara, 1997). For instance, the larger neuromasts and larger diameters that characterize widened canals (reviewed in Webb, 2013) are hypothesized to be peramorphic features, while the reduction in canal ossification that results in the large canal pores bounded by bony bridges (as opposed to a solid canal roof pierced by small pores) of widened canals are hypothesized to be a paedomorphic feature. The mechanisms underlying observed heterochronic change likely include changes in osteoblast and osteoclast activity that alter the timing and/or pattern of ossification of the canals, and/or changes in rates of hair cell differentiation from support cells that result in differences in the size and shape of hair cell populations, and thus neuromast morphology. Changes in gene expression and/or the action of gene products involved in these processes could explain differences in adult canal and neuromast morphology. Such differences are hypothesized to occur via heterochrony, but alternatively, changes in gene expression (or action of gene products) could cause dramatic morphological differences in early larvae followed by isometric increases in canal diameter and neuromast size relative to fish size.

Any study of the developmental basis for evolutionary change in phenotype requires the availability of complete ontogenetic series from closely related species that have the phenotypes of interest. The study of the development of widened lateral line canals, in particular, has been hampered by the fact that the small number of taxa with widened canals (Webb, 2014) are largely inaccessible for study and/or are particularly difficult to rear in the laboratory. The speciose and diverse cichlid fishes provide an important opportunity to test a hypothesis of

heterochrony in the evolution of the cranial lateral line system. They typically have narrow cranial lateral line canals (Tarby and Webb, 2003; Branson, 1961; Peters, 1973; Webb, 1989c), but among the endemic Lake Malawi cichlids, *Aulonocara*, *Alticorpus* and *Trematocranus* have widened lateral line canals (Konings, 1990, 2007). Like other Lake Malawi cichlids that have proven to be excellent subjects for comparative analyses of functional morphology and development (Albertson and Kocher, 2001, 2006; Albertson, et al., 2001, Streelman, et al., 2003; Hulsey et al., 2005; Sylvester et al., 2010), *Aulonocara* spp. (peacock cichlids; Meyer et al., 1987) are particularly easy to maintain and rear under laboratory conditions. Furthermore, in contrast to other cichlids, which are generally considered to be visual predators, *Aulonocara* uses its lateral line system to detect water flows generated by benthic invertebrate prey living in sandy substrates (Konings, 1990; Schwalbe, et al., 2012). In this study, a comparison of the pattern and timing of development of cranial lateral line canals and canal neuromasts in *Labeotropheus fuelleborni* and *Metriaclima zebra* (narrow canals) with *Aulonocara baenschi* (widened canals) were used to test the hypotheses that the evolution of widened canals is the result of heterochrony.

MATERIALS AND METHODS

The three study species, *Labeotropheus fuelleborni*, *Metriaclima zebra*, and *Aulonocara baenschi* (referred to by genus throughout), were reared at 27.8^{O}C with a 12:12 light cycle in a multi-tank re-circulating system. For each species, one male was placed in a tank with 4-5 females to facilitate breeding and fish were fed 2x/day with commercial flake food. Fry were extracted from the mouths of brooding females a few days after hatch and reared in small

129 containers supplied with a constant flow of tank water and after yolk absorption were fed high-
130 quality Spirulina flake food (as per Albertson and Kocher, 2001). Fish were sampled periodically
131 over two months yielding developmental series that were prepared for histological analysis,
132 SEM, and clearing and staining (Fig. 1). All fish were anaesthetized in MS222 and fixed in 10%
133 formalin in phosphate-buffered saline (PBS). All procedures followed an approved IACUC
134 protocol.
135
136 **Histological Analysis**
137 Histological material was prepared from one brood each of *Labeotropheus* (n=9, 11-70 dpf,
138 7.5-21.5 mm SL), *Metriaclima* (n=9, 11-70 dpf, 8-23 mm SL), and *Aulonocara* (n=18, 5-53 dpf,
139 <5.0-23 mm SL; Fig. 1). *Labeotropheus* and *Metriaclima* >11 mm SL were decalcified in Cal-Ex
140 (Fisher) for 4 hours (11-12 mm SL), or overnight (≥16 mm SL), then rinsed in phosphate buffer,
141 and placed for one hour each, in cold 5%, 10% and 20% sucrose solutions in PBS. *Aulonocara*
142 was decalcified for 2 hours (6.0-7.5 mm SL), 3.5 hours (8.0-8.5 mm SL) or 8 hours (>8.5 mm
143 SL). All fish were dehydrated in an ascending ethanol and t-butyl alcohol series and embedded in
144 Paraplast Plus (Fisher). Serial transverse sections were cut at 8 μm, mounted on slides subbed
145 with 10% albumen in 0.9% NaCl, and stained with a modification of the HBQ stain (Hall, 1986)
146 to accomplish differential staining of cell nuclei, cartilage and bone. The supraorbital (SO),
147 mandibular (MD), preopercular (PO) and infraorbital (IO) canals were easily observed in
148 histological sections.
149 The supraorbital (SO) and mandibular (MD) canals run rostro-caudally in the nasal and
150 frontal bones (dorsal surface of skull) and in the dentary and anguloarticular bones (lower jaw)
151 were particularly conducive to quantitative analysis histological material (also see Tarby and

Webb, 2003; Webb and Shirey, 2003). First, a complete inventory of serial transverse sections of the head in each specimen revealed canal neuromast location, and names (SO1-5, MD1-5) were assigned based on their location. Then, the pattern and timing of the development of the canal segments forming around each canal neuromast were assessed using the developmental stages defined for *Amatitlania nigrofasciata* (=*Archocentrus nigrofasciatus*, Stages I-IV; Tarby and Webb, 2003).

A quantitative analysis of the rate of neuromast growth (length and width of SO1-5, MD1-5) and increase in canal diameter (at the level of each canal neuromast) was carried out for the SO and MD canals in larvae and juveniles (5-25 mm) of all three species. This allowed a test of the hypothesis that heterochronic changes in the rates of increase in neuromast size (length, width) and canal diameter among species can explain the evolution of a widened lateral line canal system from a narrow lateral line canal system. In addition, a comparison of canal and neuromast development in the SO and MD canals in the three species was used to determine if there is evidence for regional (or local) heterochrony between the MD and SO canals. It was predicted that the MD canal would be wider, which would be consistent with the notion that the MD is an adaptation, in particular, for detection of benthic prey in *Aulonocara* (Schwalbe, et al., 2012).

Neuromast length was determined by counting the number of sections in which neuromast tissue (hair cells surrounded by thickened epithelium composed of mantle cells) was present and multiplying by section thickness (8μm; measurement error ±16μm). Neuromast width was measured (to nearest 0.1μm) at the rostro-caudal midpoint of each canal neuromast by digitally tracing the curve defined by the apical surface of the cells composing the neuromast around the inner circumference of the canal. Internal canal diameter (defined by internal surface of ossified

canal bone) was measured (to nearest 0.1μm) at the level of each neuromast in the same section as neuromast width, across the canal, at its widest point above the neuromast. Canal diameter could not be measured until canal morphogenesis had commenced, so canal diameter was determined only in those canal segments that were already at Stage II-IV. Canal diameter is known to fluctuate such that canal diameter tends to be larger between neuromast positions than at neuromast positions along the canal, especially in some (but not all) species with widened canals (Webb, 2014). Thus, by measuring diameter at the level of each neuromast, comparisons among species with narrow and widened canals are more consistent and provide a conservative measure of interspecific differences in canal diameter.

All measurements were obtained digitally using Spot software (v. 5.0, Diagnostic Instruments, Sterling Heights, MI USA) on an Olympus BH-2 or Zeiss AxioVision software (v 4.6.3, Carl Zeiss MicroImaging GmbH, Gottingen, Germany) on a Zeiss AxioImager1 compound microscope. Left-right means of values for each parameter (canal diameter, neuromast length, neuromast width) were calculated to reduce the effects of asymmetry arising with variation in plane of section among individuals. Analysis of Covariance (ANCOVA; JMP, v.10.0.2, SAS Institute, Inc.) was used to detect differences in slopes for each parameter (canal diameter, neuromast length, neuromast width) among the three species after data were tested for normality, and log transformed if needed. If slopes for a given parameter were determined to be heterogeneous (statistically different), then the Johnson-Neyman technique (Johnson and Neyman, 1936) was performed to determine the range of X values (in this case, fish size) in which there is no significant difference in the parameter of interest ("region of non-significance"; White, 2003) between two species and by extension, the range of fish sizes in which a significant difference is present. A similar analysis was then performed to detect differences ontogenetic

198 trends in neuromast size (length, width) and canal diameter in the SO versus MD canals in each
199 of the three study species using the same approach. Significance was defined a priori as $P<0.05$
200 in all analyses. The graphic representation of data is derived from raw (not log transformed data)
201 to illustrate biologically (as opposed to statistically) relevant measurements.
202
203 **Scanning Electron Microscopy**
204 Specimens of *Labeotropheus* (from two broods including that used for histological analysis,
205 7-70 dpf, 7.5-26 mm SL, n=17; Fig. 1) were dehydrated in an ascending series of ethanol, critical
206 point dried in liquid CO_2, coated with Au-Pd alloy, and mounted on carbon-coated stubs in order
207 to visualize as many of the lateral line canals as possible. Specimens were imaged with a Hitachi
208 S5-7 SEM and acquired using 4x5 Polaroid film. Photos were scanned at high resolution and
209 minimally post-processed using Adobe Photoshop 4.0 (Adobe Systems, Inc., San Jose, CA,
210 USA).
211
212 **Clearing and Staining and *μ*CT Imaging**
213 *Aulonocara baenschi* (12-39 dpf, 7-19 mm SL, n=12, from one brood; Fig. 1) were
214 enzymatically cleared and stained for both bone (Alizarin Red) and cartilage (Alcian Blue;
215 Potthoff, 1984) to visualize the lateral line canals. In addition, micro-computed tomographic
216 (*μ*CT) imaging was carried out on a formalin-fixed specimen of *Aulonocara baenschi* (87 mm
217 SL). The fish was imaged in air using tube settings of 45 kVp and 177 μA, integration time of
218 300 ms, and scan resolution (voxel size) of 6 *μ*m (smaller fish) or 16 *μ*m (larger fish) using a
219 *μ*CT 40 (Scanco Medical AG, Brütisellen, CH). Once reconstructed, 3-D image volumes were

exported as DICOM image stacks and reconstructed using volume and surface rendering protocols in OsiriX (Pixmeo, Geneva Switzerland; *http://www.osirix-viewer.com/*).

RESULTS

The timing of major developmental events was similar in all three species. Hatching occured at <7 days post-fertilization (dpf, at <5 mm TL) and newly hatched fry had a large ovoid yolk sac (Fig. 2). Caudal fin flexion started quickly, just a few days post-hatch, and was complete at 7-8 dpf (<7.5 mm SL) in *Labeotropheus* and *Metriaclima* and a few days later in *Aulonocara* (11 dpf, ~7 mm SL). In all three species, the yolk sac was not absorbed until well after flexion was complete, at 18-21 dpf (11-12 mm SL; Balon, 1977; C. Albertson, pers. comm.), just prior to the normal time of release from the mother's mouth.

Distribution of Canals and Canal Neuromasts

Labeotropheus, *Metriaclima* and *Aulonocara* have the same number of canal neuromasts and the same complement of cranial lateral line canals. Five canal neuromasts are present in the supraorbital canal (SO1-5). SO1 is located in the portion of the canal in the tubular nasal bone just medial to the naris (Fig. 4C, 5A, C) and neuromasts SO2-5 are located in the portion of the canal embedded in the frontal bone. Five canal neuromasts (MD1-5) are present in the mandibular canal (Fig. 3A-C). Neuromasts MD1-4 are in the portion of the MD canal in the dentary bone, and neuromast MD5 is located in the short canal segment in the angulo-articular bone (Fig. 3A-C, and in illustrations of *Labeotropheus* and *Metriaclima* in Albertson and Kocher (2001). In addition, the preopercular (PO) canal, which is contiguous with the MD canal, is contained in the L-shaped preopercular bone (Fig. 3A-C; Fig. 4A, B). The infraorbital (IO) canal

is contained within the lacrimal bone just under the rostro-ventral border of the orbit (Fig. 4C) and continues caudally in the series of infraorbital ossicles that follow the circumference of the orbit (Fig. 3A-C). The difference in the diameter of the IO canal in *Labeotropheus* and *Metriaclima* (Fig. 3A, B) versus *Aulonocara* (Fig. 3C). is particularly noticeable. On the dorsal surface of the head, the pore between neuromasts SO3 and SO4 in each of the SO canals extend medially to form a pore in the dorsal midline, joining the right and left SO canals (Fig. 5C, D). Finally, caudal to the orbit the post-otic canal continues through the pterotic, extrascapular, post-temporal, and supracleithral bones and is contiguous with the trunk canal contained in the lateral line scales.

Pattern and Timing of Canal Morphogenesis

In all three species, the pattern of development of individual canal segments was the same (e.g., Stages I-IV; Tarby and Webb, 2003) despite differences in canal morphology (narrow vs. widened). Initiation of canal morphogenesis, marked by the formation of longitudinal depressions or grooves in the vicinity of individual canal neuromasts (Stage II; Fig. 6B, C, G, H), started within two weeks of fertilization (at 7-8 mm SL). The processes of canal segment enclosure (Stage III; Fig. 6D, I) and ossification (Stage IV; Fig. 6E, J) then continued for many more weeks through metamorphosis (larval-to-juvenile transformation; at 10-12 mm SL), and a concurrent three-fold increase in fish size.

A comparison of the timing of canal morphogenesis showed considerable asynchrony among canals. In *Labeotropheus*, SO, MD, and PO canal grooves (Stage II) were visible as early as ~10-11 dpf (7-8 mm SL; Fig. 4A, C). Within a day (at 12 dpf), the SO and MD canals started to enclose (Stage III). Several days later (17-18 dpf, 11-12 mm SL), the PO and MD canals were

partially or completely enclosed, and the infraorbital (IO) canal (the portion in the lacrimal bone, but not the remainder of the IO canal contained within in the infraorbital ossicles) was enclosed (Fig. 4C, D). Within two days (19-20 dpf, 12 mm SL, when fish are normally ready to be released from the mother's mouth), some or all of the segments that compose each of the canals, with the exception of the portion of the IO canal in the infraorbital ossicles caudal to the lacrimal bone, had enclosed and ossification (Stage IV) had started (Fig. 5A, B). After several weeks (by 42 dpf, 16 mm SL), the SO, MD and PO canals had all ossified (Stage IV), and the IO canal segments in the infraorbital ossicles were finally enclosed (Stage III). SEM illustrated the pores in one juvenile at 56 dpf (~19 mm SL) in which the pores of adjacent canal segments that compose the IO canal had still not fused, leaving double pores (Fig. 5E) and at 70 dpf (~23 mm SL) the double pores had fused to form the single pores characteristic of adult fishes (Fig. 5F).

The timing of canal morphogenesis in *Metriaclima* appears to be similar to that in *Labeotropheus*. The SO, MD and PO grooves (Stage II) were apparent in young larvae just after flexion was complete (~11 dpf, 7-8 mm SL), and most or all of the SO and MD canal segments were enclosed (Stage III) about a week later (17-20 dpf; 11 mm SL). By 20-22 dpf (11-12 mm SL), the portion of the IO canal in the lacrimal (containing three canal neuromasts) was enclosed, but the enclosure of the remainder of the IO canal (in the infraorbital ossicles) was delayed for many weeks (Fig. 4C, 6E, F). The SO and MD canal segments were all ossified (Stage IV) in juveniles between 42 and 56 dpf (~19-20 mm SL).

In *Aulonocara*, SO grooves (Stage II) were present a bit earlier (at 8 dpf, ~5 mm SL) and some MD grooves were already present at 11 dpf (~7 mm SL) as in *Labeotropheus* and *Metriaclima*. Enclosure of the SO and MD canals (Stage III) started in slightly older individuals (15-17 dpf, 9-11 mm SL) than in *Labeotropheus* and *Metriaclima*, as yolk absorption had begun.

289 At 20-26 dpf (11-12 mm SL), the SO and MD canals, and the portion of the IO canal in the
290 lacrimal bone were enclosed and had begun to ossify (Stage IV); the SO and MD canals were
291 ossified several weeks later (47 dpf; 21-22 mm SL).
292 The onset of canal enclosure (Stage III) and canal ossification (Stage IV) in the SO and MD
293 canals showed some interesting contrasts between the species with narrow canals
294 (*Labeotropheus* and *Metriaclima*) and widened canals (*Aulonocara*). First enclosure in the SO
295 canal occurred by 11-12 dpf in *Labeotropheus* and *Metriaclima*, but occurred over a longer
296 interval (11 to 15 dpf) in *Aulonocara*. First ossification in the SO canal occurred between 12 and
297 17 dpf in *Labeotropheus* and *Metriaclima*, and a few days later (17 to 20 dpf) in *Aulonocara*.
298 Similarly, first enclosure in the MD canal occurred by ~11-12 dpf in *Labeotropheus* and
299 *Metriaclima*, and a few days later (15 to 17 dpf) in *Aulonocara*. First ossification in the MD
300 canal occured at 12 to 17 dpf in *Labeotropheus* and *Metriaclima*, but several days later (23 to 26
301 dpf) in *Aulonocara*.
302
303 **Order and Timing of Development of Segments within Canals**
304 Asynchrony in development was obvious among canal segments within a canal, but a
305 particular canal segment was not observed at all four of the developmental stages (I-IV) in
306 different individuals due to the rapid progression of canal development and the size and age of
307 individuals available for analysis. Thus, mean fish size at first canal enclosure (Stage III) and
308 canal ossification (Stage IV) for each canal segment was used to approximate the relative order
309 and timing of the development of canal segments within the SO and MD canals (Table 1).
310 The development of the segments of the SO and MD canals did not occur in a simple rostro-
311 caudal (or caudo-rostral) direction within a canal. Nevertheless, a consideration of the mean fish

312 size at which a particular canal segment enclosed and ossified among the individuals analyzed
313 revealed trends that allowed some generalizations to be made (see Table 1). In the SO canal, the
314 SO4 canal segment appeared to be the first to enclose (at ~8-9 mm SL) and the first to ossify in
315 all three species. The other segments then enclosed in a roughly caudal to rostral direction, with
316 the more caudal segments (SO3-5) tending to enclose before the more rostral segments (SO1-3).
317 Subsequent ossification occurred in roughly the same order among segments. The order and
318 timing of the enclosure and ossification of individual canal segments appears to be a bit different
319 in the MD canal. The MD2 segment tended to enclose first in *Labeotropheus*, but the MD3
320 segment tended to enclose first in *Metriaclima* and *Aulonocara*. The order of ossification did not
321 reveal any particular pattern in *Labeotropheus*, but in *Metriaclima* and *Aulonocara*, the more
322 caudal segments (MD3-5) enclosed before the more rostral segments (MD1-2).
323
324 **Canal Diameter at Enclosure and Ossification**
325 Canal diameter could be measured as soon as a neuromast had sunk into a depression or
326 groove (Stage II, Fig. 6B, G). Canal diameter continued to increase as bone ossified to form the
327 canal walls (Fig. 6C, H), as the canal enclosed (Stage III, Fig. 6D, I), and as the canal roof
328 ossified (Stage IV; Fig. 6E, J). The minimum canal diameters for each SO and MD canal
329 segment at first enclosure (Stage III) and ossification (Stage IV) provided insights into the
330 functional implications of canal growth during larval and juvenile development (Table 1). In
331 *Labeotropheus* and *Metriaclima* (narrow canals) the SO and MD canal segments were first
332 enclosed at diameters of at least ~65 and ~95 μm, respectively, but in *Aulonocara* (widened
333 canals) they enclosed at diameters of at least ~70 and ~115 μm, respectively. Thus, the MD
334 canal segments tended to enclose at larger diameters than those of the SO canal in all three

species and the MD canal in *Aulonocara* tended to enclose at larger diameters than in either *Labeotropheus* or *Metriaclima*. Ossification occurred at diameters of at least 20 μm, but in some cases, 60 μm greater than the diameters at which enclosure was observed in a particular MD canal segment. The minimum diameter at which the five MD segments ossified was 83-109 μm in *Labeotropheus* (versus 78-120 μm for its five SO segments), 108-170 μm in *Metriaclima* (versus 81-119 μm for its SO segments) and 136-194 μm in *Aulonocara* (versus 93-183 μm for its SO segments).

Quantitative Analysis of Neuromast and Canal Development

An ANCOVA (SO and MD canal data combined) revealed that rates of increase in canal diameter and neuromast size (length, width) varied significantly among species (Fig. 7, Table 2). However, significant interactions (species x fish size) were found for neuromast size (length and width) and canal diameter, so the Johnson-Neyman technique (White, 2003) was used to determine the range of fish sizes in which each parameter was not statistically different (between species pairs), and thus by extension when it was statistically different ($P<0.05$).

The ontogenetic rate of increase in canal diameter was not statistically different (equal slopes) in *Labeotropheus* and *Metriaclima*, but canal diameters were consistently larger in *Metriaclima* (Table 2). The rate of increase in canal diameter in *Aulonocara* was 1.5 and 1.9 times that in *Labeotropheus* or *Metriaclima*, respectively (Fig. 7A; Table 2, 3). As a result, canal diameter was already significantly larger in *Aulonocara* than in either *Labeotropheus* or *Metriaclima* larvae at lengths >4.5 and >7.8 mm SL, respectively.

Similarly, the ontogenetic rate of increase in neuromast length was not statistically different in *Labeotropheus* and *Metriaclima*, but neuromasts were consistently longer in *Labeotropheus*

than in *Metriaclima* (Fig. 7B; Table 2, 3). In *Aulonocara*, neuromast length increased at a rate that was 2.7 or 2.8 times that in *Labeotropheus* or *Metriaclima*, respectively (Table 3) and neuromast length was significantly greater in *Aulonocara* than in either *Labeotropheus* or *Metriaclima* larvae at lengths >12.3 and >9.0 mm SL, respectively. The ontogenetic rate of increase in neuromast width was not statistically different in *Labeotropheus* and *Metriaclima*, but neuromast width was consistently greater in *Metriaclima* (Fig. 7C). Neuromast width in *Aulonocara* increased at a rate 2.2 or 1.6 times that in *Labeotropheus* or *Metriaclima*, respectively (Table 2) and was significantly greater in *Aulonocara* larvae than in either *Labeotropheus* or *Metriaclima* larvae at lengths >8.3 and >7.6 mm SL, respectively.

Another ANCOVA revealed differences in rates of increase in canal diameter and neuromast size (length, width) in the supraorbital (SO) versus the mandibular (MD) canal in the three study species (Table 4, 5). In *Labeotropheus*, canal diameter and neuromast length increased at rates that were not statistically different in the SO and MD canals, but SO canals were wider and SO neuromasts were longer than the MD canal and MD canal neuromasts (Table 4). The rate of increase in neuromast width was 1.8 times greater in the SO canal than in the MD canal (Table 5), such that neuromasts were significantly wider in the SO canal than in the MD canal in larvae >9.7 mm SL. In *Metriaclima*, neuromast length in the two canals increased at rates that were not statistically different (Table 4), but neuromasts were consistently longer in the SO canal. The rates of increase of neuromast width and canal diameter were greater in the SO canal in *Metriaclima* by a factor of 2.1 and 1.6, respectively (Table 5), such that SO neuromast width was significantly greater in larvae >16.0 mm SL, and SO canal diameter was significantly greater in larvae >14.1 mm SL. In *Aulonocara*, canal diameter and both neuromast length and width all increase faster in the SO canal than in the MD canal (Table 4), which was unexpected. Canal

diameter increased 1.3 times faster in the SO canal than in the MD canal (Table 5), such that the SO canal was significantly wider than the MD canal in larvae >15.2 mm SL. Neuromast length and width both increased 1.2 times faster in the SO canal (Table 5) such that SO neuromasts were significantly longer and wider than MD neuromasts in larvae at lengths >12.3 mm SL and >9.6 mm SL, respectively. The differences in developmental rate between the SO and MD canal can be attributed to regional (local) heterochrony.

DISCUSSION

This study has provided the first detailed description of the development of widened lateral line canals in a teleost, and the first detailed comparison of the development of narrow and widened canals. It has shown that: 1) canal neuromast number and the pattern of canal morphogenesis are conserved, regardless of adult canal morphology, 2) the evolution of widened canals from narrow canals can occur via dissociated heterochrony (a combination of peramorphic and paedomorphic trends) and regional (local) heterochrony in canal diameter and neuromast size between canals accounts for variation among canals within a species, and 3) the morphology of the lateral line canals and the dermal bones in which they are found (e.g., the mandibular canal contained within the dentary and anguloarticular bones of the mandible) can evolve independently of each other.

Pattern and timing of development in narrow versus widened canals

The three study species (*Labeotropheus fuelleborni, Metriaclima zebra*, *Aulonocara baenschi*) had the same complement of canal neuromasts in the SO and MD canals. This is evidence of a conserved process of neuromast patterning that is independent of the subsequent

development of the lateral line canals. In addition, the same pattern of development was observed in the three study species and occurs in four stages as described in a South American cichlid with narrow canals (*Amatitlania nigrofasciata = Archocentrus nigrofasciatus*; Tarby and Webb, 2003), and an unrelated teleost, the zebrafish, *Danio rerio* (Webb and Shirey, 2003). Thus, the pattern of groove formation (Stage II), enclosure (Stage III) and canal roof ossification (Stage IV) that results in the formation of lateral line canal segments appears to be conserved among teleosts with both narrow and widened canals.

The timing of the different stages of canal development varies among species (Tarby and Webb, 2003; Webb and Shirey, 2003) and may be related to functional demands in developing fishes (Webb, 2013). For instance, the morphogenesis of the cranial lateral line canals progresses quickly to Stage IV (ossification of enclosed canal segments) in both the African cichlids examined in this study and the South American convict cichlid examined in a prior study (*Amatitlania nigrofasciata*; Tarby and Webb, 2003). The result is that in *Labeotropheus*, *Metriaclima* and *Aulonocara*, canal enclosure (Stage III) and ossification (Stage IV) is well-underway after a prolonged process of yolk absorption when transforming juveniles are normally released from the mother's mouth, and must start to feed (at ~ 21 days post-fertilization). In contrast, the cranial lateral line canals in larval and juvenile zebrafish demonstrates a prolonged stage II, in which presumptive canal neuromasts sit in open grooves (Webb and Shirey, 2003). This morphology is predicted to facilitate detection of prey at the water's surface in their native habitat, as has been demonstrated in killifish (Schwarz, et al., 2011).

The quantitative ontogenetic analysis presented here has demonstrated that canal diameter and neuromast size are initially similar among the three study species, but that significantly different rates of increase in these parameters result in the development of narrow canals

(*Labeotropheus and Metriaclima*) versus widened canals (*Aulonocara*). In addition, the process of canal enclosure in the SO and MD canals commences a bit later and the process is a bit more prolonged (over a longer growth interval) and occurs at larger canal diameters in *Aulonocara* in contrast to the narrow canals of *Labeotropheus* and *Metriaclima*. Nevertheless, by the time larvae are normally released from the mother's mouth (~ 21 dpf; 11-12 mm SL), canal diameter (Fig. 4e, j) and neuromast length and width already distinguish *Aulonocara* (widened canals) from *Labeotropheus* and *Metriaclima* (narrow canals).

Interspecific differences in lateral line morphology are correlated with differences in feeding habit. *Labeotropheus* feeds on filamentous algae from rocks and *Metriaclima* brushes loose plant matter from algae beds, but also plucks plankton from the water column (Albertson and Kocher, 2006), and it is likely that the lateral line system is not critical for feeding in these taxa. However, *Aulonocara stuartgranti* uses its widened lateral line canal system to detect benthic invertebrate prey as it swims and glides over sandy substrates (Schwalbe et al., 2012). Its feeding behavior suggests that the MD canal, lower arm of the PO canal, and perhaps the portion of the IO canal ventral to the orbit (whose pores are obvious in ventral view, Fig. 3) are critical for prey detection. Surprisingly, the SO canal increases in diameter faster than the MD canal such that the SO canal is wider in diameter and its canal neuromasts are longer and wider than those in the MD canal in all three study species, regardless of canal morphology. Thus, the prediction that canal diameter and neuromast size in the MD canal would be greater than in the SO canal as the result of adaptive function for benthic prey detection was not borne out. Nevertheless, in *Aulonocara*, the MD canal enclosed and was ossified at diameters >100 μm and canal diameter and was already larger than in *Labeotropheus* or *Metriaclima* in early larvae (lengths >7.8 mm SL), such that the widened MD canal becomes morphologically

distinguishable from the narrow MD canal well before feeding commences. The timing of the onset of lateral line-mediated feeding behavior (as described in adults, Schwalbe et al., 2012) is not yet known, but it is predicted that it will be dependent on the development of their typical prey search strategy (three phase cycle: swim, glide, pause) as well as favorable hydrodynamic properties of the lateral line canals that will allow stimulation of canal neuromasts by the water flows generated by prey.

It is concluded that the evolution of widened canals and their larger canal neuromasts are the result of dissociated heterochrony. High rates of increase in canal diameter and neuromast size are interpreted as peramorphic trends and the delay of SO and MD canal enclosure and the prolonged duration of this process in *Aulonocara* in contrast to *Labeotropheus* and *Metriaclima* are interpreted to be paedomorphic trends. In addition, the initial process of canal roof ossification and fusion of adjacent canal segments to form a common pore is followed by a decrease in pore size in *Labeotropheus* (Fig. 5C, D and Fig. 5E, F), a process noted by Allis (1889) in *Amia calva*. Thus, the evolution of large canal pores characteristic of widened canals (Webb, 1989b) appears to be the result of a paedomorphic trend - either a slower rate in, or truncation of the process of ossification of the canal roof in comparison to that in species with well-ossified narrow canals that have smaller canal pores.

The Mandibular Lateral Line Canal as a Component of the Mandible

Labeotropheus and *Metriaclima* are distinguished by the morphology and genetics of the oral jaw apparatus, including differences in the length and width of the lower jaw (Albertson and Kocher, 2006), which are attributed to directional selection (Albertson, et al., 2003). A QTL analysis had indicated that several aspects of mandibular morphology critical for feeding are

473 inherited as modules, thus supporting the notion of a degree of morphological integration in the
474 cichlid mandible (Albertson and Kocher, 2006). However, the function of the mandible is not
475 limited to feeding and it is thus subjected to other selective pressures, such as those associated
476 with lateral line function. This study has shown that the diameter of the MD canal and size of the
477 canal neuromasts contained within it are not significantly different in *Labeotropheus* and
478 *Metriaclima* in mid-stage larvae and older or larger individuals, despite significant differences in
479 overall mandibular morphology (Konings, 1990). The mandibular canal is narrow and well-
480 ossified in both species, with the same number of canal neuromasts and small canal pores.
481 Interestingly, the canal pores in the shortened mandible of *Labeotropheus* appear to be more
482 closely positioned to each other than those in *Metriaclima* (as in Fig. 3 and illustrations in
483 Albertson and Kocher, 2001). This difference in inter-pore distance, presumably related to
484 differences in mandibular length, may have unappreciated consequences for the lateral line
485 function (discussed in Coombs and van Netten, 2006).
486 If the mandible can respond to directional selection with respect to feeding while the MD
487 canal does not change in diameter, then it follows that the morphology of the MD canal could
488 evolve independently of lower jaw morphology in response to selection for modified water flow
489 detection. For example, the morphology of the lower jaw of *Aulonocara* spp. (Fig. 3a, b) appears
490 to be similar to that in *Metriaclima*, but this study has shown that while neuromast patterning
491 (number of canal neuromasts) does not differ between these two taxa, canal width and neuromast
492 size diverge in larval *Aulonocara* and *Metriaclima*, to become the widened and narrow lateral
493 line canals characteristic of juveniles and adults (Fig. 6E, J). The evolution of widened canals
494 from narrow canals for the enhancement of prey detection capabilities may also have impacts on
495 lower jaw function. Examination of dried skeletons revealed that the mandible of *Aulonocara*

496 appears particularly "delicate" (Webb and Kocher, unpubl. observ.) due to reduced ossification
497 of the canal roof resulting in their characteristically large pores, but the consequences of these
498 features for feeding mechanics have not been considered. A consideration of the lateral line
499 canals as components of the dermatocranial bones, with functional roles (e.g., ventrally directed
500 canals in benthic feeders) or more subtle architectural or constructional roles (e.g., the dorsal SO
501 canal in the frontal bone), is an aspect of the analysis of the integration and modularity in the
502 skull of fishes that deserves more attention.
503

504 ## Summary

505 This study has demonstrated that simple, correlated changes in developmental rates
506 (heterochrony) in the lateral line canals contained within dermal bones (a component of the
507 dermatocranium) and in canal neuromasts (a component of the peripheral nervous system) can
508 explain the evolution of an adaptive phenotype, widened lateral line canals. In particular, it
509 revealed "dissociated heterochrony" among species with narrow vs. widened canals (a
510 combination of peramorphic and paedomorphic shifts), as well as regional (local) heterochrony,
511 differences in rates between canals (and between their respective neuromasts) within individuals.
512 The genetic basis of these changes deserve further study and will need to consider the processes
513 of intramembranous bone ossification and dynamics of hair cell populations in neuromasts. This
514 study also demonstrated that heterochronic change in canal diameter and neuromast morphology
515 can occur without a change in other aspects of lateral line development (e.g., neuromast
516 patterning [canal neuromast number] or the pattern/process of neuromast-centered canal
517 morphogenesis). With reference to the life history of the mouth brooding cichlid fishes used in
518 this study, the divergence in canal phenotype (narrow vs. widened) has already occurred in

519 young larvae, so that by the time they are released from the mother's mouth and exogenous
520 feeding commences, canal diameter and neuromast size already distinguish *Aulonocara*
521 (widened canals) from *Labeotropheus* and *Metriaclima* (narrow canals), which is likely to have
522 interesting implication for the ontogeny of prey detection capabilities. Finally, the ability of the
523 lower jaw to evolve independently of lateral line canal morphology (*Labeotropheus* vs.
524 *Metriaclima*), and the ability of the lateral line canals (and neuromasts) to evolve independently
525 of the lower jaw (*Aulonocara* vs. *Metriaclima*), demand that the canals of the mechanosensory
526 lateral line system become a part of the conversation concerning integration and modularity in
527 the skull of fishes.
528

529 ## ACKNOWLEDGMENTS

530 We thank Thomas Kocher, Karen Carleton and Craig Albertson for providing the specimens
531 used in this study. Morgan Falk did a portion of the initial histological analysis as part of her
532 Senior Honors Thesis at Villanova University. Douglas Moore (Orthopedics Research Lab, RI
533 Hospital/Brown Medical School) carried out μCT scans and Timothy Alberg generated 3-D
534 images from μCT data. Jason Kolbe provided statistical expertise. The initial preparation of
535 histological and SEM material was supported by an NSF Research Opportunity Award to JFW as
536 a supplement to NSF grant DEB-9905127 to Thomas Kocher. Completion of this work was
537 supported by the College of the Environment and Life Sciences, University of Rhode Island and
538 NSF Grant No. 0843307 to JFW.
539

540 ## LITERATURE CITED

541 Albertson RC, and Kocher TD. 2001. Assessing morphological differences in an adaptive trait: A

542 landmark-based morphometric approach. J Exper Zool 289:385-403.
543 Albertson RC, and Kocher TD. 2006. Genetic and developmental basis of cichlid trophic
544 diversity. Heredity 97:211-21.
545 Albertson RC, Streelman JT, and Kocher TD. 2003. Genetic basis of adaptive shape differences
546 in the cichlid head. J Heredity 94:291-301.
547 Allis EP. 1889. The anatomy and development of the lateral line system in *Amia calva*. J
548 Morphol 2:463–542+ plates.
549 Aman A, and Piotrowski T. 2011. Cell-cell signaling interactions coordinate multiple cell
550 behaviors that drive morphogenesis of the lateral line. Cell Adh Migr 5:499-508.
551 Balon EK. 1977. Early ontogeny of *Labeotropheus* Ahl, 1927 (Mbuna, Cichlidae, Lake
552 Malawi), with a discussion of advanced protective styles in fish reproduction and
553 development. Env Biol Fishes 2:147-176.
554 Branson BA. 1961. The lateral-line system in the Rio Grande Perch, *Cichlasoma cynoguttatum*
555 (Baird and Girard). Amer Midl Nat 65:446-458.
556 Chitnis AJ, Nogare DD, and Matsuda M. 2011. Building the posterior lateral line system in
557 zebrafish. Devel Neurobiol 72:234–255.
558 Coombs S and Van Netten S. 2006. The hydrodynamics and structural mechanics of the lateral
559 line system. In: Shadwick RE and Lauder GV editors, Fish Biomechanics, San Diego:
560 Elsevier Academic Press. pp. 103-139.
561 Denton EJ and Gray JAB. 1988. Mechanical factors in the excitation of the lateral lines of fish.
562 In: Atema J, Fay RR, Popper AN, and Tavolga WN, editors. Sensory Biology of Aquatic
563 Animals. New York: Springer-Verlag. pp. 595-617.

564 Denton EJ and Gray JAB. 1989. Some observations on the forces acting on neuromasts in fish
565 lateral line canals. In: Coombs, S, Görner P, and Munz H, editors. The Mechanosensory
566 Lateral Line: Neurobiology and Evolution. New York: Springer-Verlag. pp. 229-246.
567 Hall BK. The role of movement and tissue interactions in the development and growth of bone
568 and secondary cartilage in the clavicle of the embryonic chick. J Emb Exper Morphol
569 93:133-152.
570 Hulsey D, Fraser GJ, and Streelman JT. 2005. Evolution and development of complex
571 biomechanical systems: 300 million years of fish jaws. Zebrafish 2:243-257.
572 Johnson PO and Neyman J. 1936. Tests of certain linear hypotheses and their application to
573 some educational problems. Stat Res Mem 1:57-93.
574 Konings A. 1990. Ad Koning's Book of Cichilds and Other Fishes of Lake Malawi. Neptune
575 City, NJ: TFH Publications.
576 Konings A. 2007. Malawi Cichlids in Their Natural Habitat, 4th ed. El Paso, Texas: Cichlid
577 Press.
578 McNamara KJ. 1997. *Shapes of Time – The Evolution of Growth and Development*. Baltimore:
579 The Johns Hopkins University Press.
580 Meyer MK, Riehl R, and Zetzsche H. 1987. A revision of the cichlid fishes of the genus
581 Aulonocara Regan, 1922 from Lake Malawi, with descriptions of six new species (Pisces,
582 Perciformes, Cichlidae). Cour Forsch-Inst Senckenberg 94:7-53.
583 Moore ME, and Webb JF. 2008. Dermal bone remodeling in the cranial lateral line canals of
584 zebrafish: The role of osteoclasts. Integr Comp Biol 47:e142.

585 Nuñez, BA, Sarrazin AF, Cubedo N, Allende ML, Dambly-Chaudière C, and Ghysen A. 2009.
586 Postembryonic development of the posterior lateral line in the zebrafish. Evol Devel
587 11:391-404.
588 Peters HM. 1973. Anatomie und Entwicklungsgeschichte des Laterallissystems von Tilapia
589 (Pisces, Cichlidae). Z Morph Tiere 74:89-161.
590 Potthoff T. 1984. Clearing and staining technique. In: Moser, JG, editor-in-chief. Ontogeny and
591 Systematics of Fishes. Special Publication No. 1. Lawrence, Kansas: American Society of
592 Ichthyologists and Herpetologists. pp. 35-37.
593 Schwalbe MAB, Bassett DK, and Webb JF. 2012. Feeding in the dark: Lateral line mediated
594 feeding behavior in the peacock cichlid, *Aulonocara stuartgranti*. J Exp Biol 215:2060-
595 2071.
596 Schwarz JS, Reichenbach T, Hudspeth AJ. 2011. A hydrodynamic sensory antenna used by
597 killifish for nocturnal hunting. J Exper Biol 214:1857-1866.
598 Streelman JT, Webb JF, Albertson RC and Kocher TC. 2003. The cusp of evolution and
599 development: a model of cichlid tooth shape diversity. Evol Devel 5:600-608.
600 Sylvester JB, Rich CA, Loh Y-HE, van Staaden MJ, Fraser GJ and Streelman JT. 2010. Brain
601 diversity evolves via differences in patterning. Proc Nat Acad Sci US 107:9718-9723.
602 Tarby ML and Webb JF. 2003. Development of the supraorbital and mandibular lateral line
603 canals in the cichlid, *Archocentrus nigrofasciatus*. J Morphol 255:44-57.
604 Webb, JF. 1989a. Developmental constraints and evolution of the lateral line system in teleost
605 fishes. In: Coombs, S, Görner P, and Munz H, editors. The Mechanosensory Lateral Line:
606 Neurobiology and Evolution. New York: Springer-Verlag. pp. 79-98.

607 Webb JF. 1989b. Gross morphology and evolution of the mechanosensory lateral line system in
608 teleost fishes. Brain Behav Evol 33:34-53.
609 Webb JF. 1989c. Neuromast morphology and lateral line trunk ontogeny in two species of
610 cichlids: an SEM study. J Morphol 202:53-68.
611 Webb JF. 1990. Ontogeny and phylogeny of the trunk lateral line system in cichlid fishes. J Zool,
612 London 221:405-418.
613 Webb JF. 2014. Morphological diversity, development, and evolution of the mechanosensory
614 lateral line system. In: Coombs S and Bleckmann, H, editors. *The Lateral Line*. New York:
615 Springer-Verlag. pp. 17-72.
616 Webb JF and Northcutt RG. 1997. Morphology and distribution of pit organs and canal
617 neuromasts in non-teleost bony fishes. Brain Behav Evol 50:139-151.
618 Webb JF and Shirey JE. 2003. Post-embryonic development of the lateral line canals and
619 neuromasts in the zebrafish. Devel Dynam 228:370-385.
620 Webb JF, Montgomery J, and Mogdans, J. 2008. Mechanosensory lateral line and fish
621 bioacoustics. In: Webb JF, Fay RR, Popper AN, editors. Fish Bioacoustics. New York:
622 Springer-Verlag. pp. 145-182.
623 White CR. 2003. Allometric analysis beyond heterogeneous regression slopes: Use of the
624 Johnson-Neyman technique in comparative biology. Physiol Biochem Zool 76:135-140.
625
626
627

Figure Captions

Fig. 1. Fish age and size for specimens of *Labeotropheus fuelleborni* (n=25), *Metriaclima zebra* (n= 8), and *Aulonocara baenschi* (n= 57) used for histological analysis, and for SEM and clearing and staining, as noted.

Fig. 2. Larval and juvenile *Aulonocara baenschi*. **A:** Yolk sac larvae (pre-flexion) on day of hatch (5.5 mm SL, 5 dpf). **B:** Yolk sac larvae (post-flexion) several days after hatch (5.5 mm SL, 8 dpf). **C:** Older yolk sac larva - cranial lateral line canals have started to develop (7 mm SL, 12 dpf). **D:** Juvenile after release from mother's mouth (14 mm SL, 29 dpf).

Fig. 3. MicroCT images of adults of the three study species. **A:** *Labeotropheus fuelleborni* (~80 mm SL, narrow canals; 1 μm resolution). **B:** *Metriaclima zebra* (~92 mm SL, narrow canals; 18 μm resolution). **C, D:** *Aulonocara baenschi* (86 mm SL, widened canals; 16 μm resolution). **A-C:** 3-D volume rendering in ventral view showing the MD, PO and IO canals. Asterisks (*) indicate the location of the canal neuromasts in the MD canal, which is contained in the dentary and angulo-articular bones (in A and B) and the canal neuromasts in the MD canal as well as in the lower arm of the L-shaped PO canal (in C). **D:** Transverse slice (16μm thickness) of *Aulonocara baenschi* at the level of the lens of the eye (e), indicating the lumen of the SO canal and the PO, IO and SO canals.

Fig. 4. Scanning electron microscopic (SEM) images illustrating canals and neuromasts of larval and juvenile *Labeotropheus fuelleborni*. **A:** Yolk sac larva (10 dpf) with very small presumptive canal neuromasts (arrows), and grooves (Stage II) of developing mandibular (MD)

and preopercular (PO) canals, n = naris. **B:** Enlargement of PO groove in A indicating oval canal neuromasts (white arrows) and two neuromasts that will remain superficial (black arrows). **C:** Early juvenile (17 dpf) with rostral portion of IO canal (in lacrimal bone), SO and PO canals that are enclosed. The other neuromasts of the IO canal series along the ventral and caudal boundaries of the orbit are still superficial (arrows). The supraorbital (SO) and preopercular (PO) canals are already enclosed and have pores. Lower jaw had been removed. **D:** Rostral-most IO neuromast (at asterisk in C) demonstrating oval shape and narrow sensory strip containing sensory hair cells each with a long kinocilium and shorter stereocilia (white strands). Double arrow indicates hair cell orientation. Neuromast is surrounded by squamous epithelial cells with prominent microvillar ridges. Scale bars in A, C = 500 μm; B = 100 μm; D = 10 μm.

Fig. 5. Scanning electron microscopic (SEM) images illustrating enclosure of canals and pores in *Labeotropheus fuelleborni*. **A:** Dorsal view of the head in a late stage larva (12 dpf), showing grooves of partially enclosed bilateral supraorbital (SO) canals. n=naris. **B:** Ventral view of mandible in a young juvenile (17 dpf) showing neuromast (left most arrow) and developing canal. **C:** Dorsal view of head of young juvenile (17 dpf) showing naris (n) and SO canal pores medial to naris and orbit (arrows). Superficial neuromasts (sn) are visible between the left and right SO canals. Note double pore at dorsal midline (mp). **D:** Dorsal view of head in larger juvenile (20 dpf), with labeling as in C. The fusion of the double pore (in C) forms a single median pore (mp). **E:** Lateral view of enclosed SO PO, and IO canals with single and double pores (arrows) in a 56 dpf juvenile. **F:** Lateral view of a 70 dpf juvenile in which the double pores in E (arrows) have fused to form smaller, single pores. Scale bars in A = 300 μm; B = 150 μm; C = 250 μm; D, E = 500 μm; F = 600 μm.

Fig. 6. Development of individual canal segments at the level of canal neuromasts in the MD canal in two species with narrow and widened lateral line canals. See text for more explanation. **A-E:** *Labeotropheus fuelleborni* (narrow canals, 17-70 dpf), **F-J:** *Aulonocara baenschi* (widened canals, 17-47 dpf). **A, F:** Stage I - neuromasts sits flush with epithelium, b, g) Stage IIa - neuromast sits in epithelial depression. **C, H:** - Stage IIb - neuromast sits in epithelial groove between ossified canal walls (pink = ossified bone). **D, I:** - Stage III - neuromast enclosed by soft tissue, E, J) - Stage IV - neuromast enclosed in ossified canal segment. m -Meckel's cartilage (turquoise) in A and other images. Arrows point to center of hair cell population in each neuromast. Note the much larger canal diameter in J (*Aulonocara,* 47 dpf) when compared to E (*Labeotropheus*, 70 dpf). Scale for all images (as in J) = 100 μm.

Fig. 7. Rates of increase in **A:** canal diameter, **B:** neuromast length, **C:** neuromast width relative to fish size (SL) in *Labeotropheus fuelleborni* and *Metriaclima zebra* (both with narrow canals) and *Aulonocara baenschi* (widened canals) derived from histological material (raw data, not log transformed is illustrated). Each data point is the mean of left and right for each neuromast or canal diameter, and data for SO and MD canals are combined. See Tables 2 and 3 for statistical analyses of log transformed data (where warranted).

TABLE 1. Mean fish size and minimum canal diameter at which individual canal segments in the supraorbital (SO) and mandibular (MD) canals are enclosed (Stage III) and ossified (Stage IV) derived from histological material. Ascending values of mean fish size at enclosure and ossification among segments within a canal series are used to infer the order of canal enclosure and ossification within that canal (see text for additional details).

		Enclosure (Stage III)		Ossification (Stage IV)	
Species	NM	Mean Fish Size (mm SL)	Min. Canal Diameter (μm)	Mean Fish Size (mm SL)	Min. Canal Diameter (μm)
Labeotropheus fuelleborni	SO1	11.8	78.4	19.0	99.1
	SO2	10.9	79.9	14.8	119.4
	SO3	10.3	106.8	14.2	77.5
	SO4	8.5	103.3	13.9	81.1
	SO5	12.0	66.8	14.2	86.5
	MD1	11.6	98.6	16.3	82.8
	MD2	10.9	36.7*	15.5	102.9
	MD3	12.0	93.9	16.0	109.4
	MD4	11.5	109.7	16.7	94.3
	MD5	11.8	93.0	19.0	97.2
Metriaclima zebra	SO1	13.2	70.4	19.2	83.9
	SO2	12.3	102.0	21.0	176.1
	SO3	11.8	69.1	21.1	182.7
	SO4	9.3	70.1	16.9	89.7
	SO5	11.5	113.1	16.9	86.7
	MD1	13.7	89.1	17.0	108.4
	MD2	12.0	85.9	21.0	169.9
	MD3	10.8	97.3	20.7	113.6
	MD4	11.3	124.8	20.7	122.7
	MD5	11.4	121.3	20.7	161.3
Aulonocara baenschi	SO1	16.1	125.9	19.0	98.2
	SO2	14.8	130.3	19.9	249.4
	SO3	13.7	111.5	18.5	183.2
	SO4	9.0	67.1	16.8	93.7
	SO5	9.3	93.0	17.5	154.8
	MD1	16.2	134.7	21.7	194.0
	MD2	16.9	115.5	15.7	166.0
	MD3	10.5	118.8	18.2	136.3
	MD4	13.7	131.1	19.9	157.4
	MD5	13.5	128.8	20.2	160.5

* obvious outlier

TABLE 2. Results of ANCOVA's for mean (left/right) canal diameter, neuromast length and neuromast width (µm) for both SO and MD canals (combined) in the three study species. All data was log transformed to achieve normality. SL = Standard length (fish size) in mm. Significance = P<0.05. See Table 3 for ANOVA results. If the interaction term for the ANCOVA was significant (indicating heterogeneity of slopes), the Johnson-Neyman technique was used to determine the region of non-significance for fish size (SL). See text for additional details.

	N	***R²***	***F***	**d.f.**	***P*-value**
Canal Diameter	280	0.77			
Species			104.0364	2, 274	<0.0001
SL			360.3079	1, 274	<0.0001
Species x SL			17.9530	2, 274	<0.0001
Neuromast Length	312	0.70			
Species			59.6912	2, 306	<0.0001
SL			221.3197	1, 306	<0.0001
Species x SL			46.1167	2, 306	<0.0001
Neuromast Width	312	0.75			
Species			81.7744	2, 306	<0.0001
SL			356.7013	1, 306	<0.0001
Species x SL			24.2879	2, 306	<0.0001

TABLE 3. Results of ANOVA showing ontogenetic trends for mean (left/right) canal diameter, neuromast length and neuromast width (µm) of SO and MD canals combined in the three study species. All data was log transformed to achieve normality. SL = standard length (fish size) in mm. See Table 2 for results of ANCOVA for these data. Significance level = P<0.05.

	N	**Regression**	**R^2**	***P***
Canal Diameter				
Labeotropheus	77	logY=1.759+0.022*SL	0.36	<0.0001
Metriaclima	80	logY=1.858+0.018*SL	0.53	<0.0001
Aulonocara	123	logY=1.781+0.033*SL	0.80	<0.0001
Neuromast Length				
Labeotropheus	77	logY=1.718+0.016*SL	0.19	<0.0001
Metriaclima	85	logY=1.623+0.015*SL	0.27	<0.0001
Aulonocara	150	logY=1.425+0.043*SL	0.80	<0.0001
Neuromast Width				
Labeotropheus	77	logY=1.574+0.021*SL	0.34	<0.0001
Metriaclima	85	logY=1.497+0.029*SL	0.59	<0.0001
Aulonocara	150	logY=1.427+0.045*SL	0.78	<0.0001

TABLE 4. Results of the ANCOVA for comparison of canal diameter, neuromast length and neuromast width (µm) in the supraorbital (SO) and mandibular (MD) canals in each of the three study species. Data was log transformed where appropriate to achieve normality. SL (Standard Length) = fish size in mm. Significance level = P<0.05. See Table 5 for ANOVA results. If the interaction term was significant (indicating heterogeneity of slopes), the Johnson-Neyman technique was used to determine the region of non-significance for fish size (SL). See text for additional details.

	N	***R²***	***F***	**d.f.**	***P*-value**
Labeotropheus					
Canal Diameter	77	0.403			
SL			45.3922	1,73	<0.0001
Canal			5.2392	1,73	0.0250
SL x Canal			0.0406	1,73	0.8408
Neuromast Length	77	0.407			
SL			25.8146	1,73	<0.0001
Canal			24.2579	1,73	<0.0001
SL x Canal			1.4813	1,73	0.2275
Neuromast Width	77	0.558			
SL			61.6011	1,73	<0.0001
Canal			26.4280	1,73	<0.0001
SL x Canal			5.3971	1,73	0.0230
Metriaclima					
Canal Diameter	80	0.575			
SL			94.7149	1,76	<0.0001

Canal			3.6308	1,76	0.0605
SL x Canal			4.6918	1,76	0.0334
Neuromast Length	85	0.302			
SL			32.039	1,81	<0.0001
Canal			2.8567	1,81	0.0948
SL x Canal			0.3114	1,81	0.5784
Neuromast Width	85	0.639			
SL			129.9772	1,81	<0.0001
Canal			0.7738	1,81	0.3816
SL x Canal			10.7873	1,81	0.0015
Aulonocara					
Canal Diameter	123	0.851			
SL			643.0620	1,119	<0.0001
Canal			5.8674	1,119	0.0169
SL x Canal			8.4776	1,119	0.0043
Neuromast Length	150	0.868			
SL			946.9223	1,146	<0.0001
Canal			9.2902	1,146	0.0027
SL x Canal			6.3914	1,146	0.0125
Neuromast Width	150	0.826			
SL			668.7916	1,146	<0.0001
Canal			19.1464	1,146	<0.0001
SL x Canal			4.4107	1,146	0.0374

TABLE 5. ANOVAs showing ontogenetic trends for mean (left/right) measurements of canal diameter, neuromast length and neuromast width in the supraorbital (SO) versus the mandibular (MD) canals of each of the three study species. Data was log transformed where necessary to achieve normality. See Table 4 for results of ANCOVA for these data. SL = standard length (fish size) in mm. Significance level = P<0.05.

		N	**Regression**	**R^2**	***P***
Labeotropheus					
Canal Diameter	SO	40	logY=1.790+0.022*SL	0.537	<0.0001
	MD	37	logY=1.715+0.023*SL	0.297	<0.0005
Neuromast Length	SO	40	Y=43.766+4.294*SL	0.281	<0.0004
	MD	37	Y=41.119+2.635*SL	0.274	<0.0009
Neuromast Width	SO	40	Y=19.519+4.754*SL	0.524	<0.0001
	MD	37	Y=30.783+2.582*SL	0.387	<0.0001
Metriaclima					
Canal Diameter	SO	39	logY=1.78+0.021*SL	0.583	<0.0001
	MD	41	logY=1.93+0.014*SL	0.530	<0.0001
Neuromast Length	SO	43	logY=1.624+0.017*SL	0.297	<0.0002
	MD	42	logY=1.620+0.014*SL	0.272	<0.0004
Neuromast Width	SO	43	logY=1.396+0.037*SL	0.776	<0.0001
	MD	42	logY=1.605+0.020*SL	0.395	<0.0001
Aulonocara					

Canal Diameter	SO	65	Y=-29.894+15.846*SL	0.841	<0.0001
	MD	58	Y=8.986+12.582*SL	0.875	<0.0001
Neuromast Length	SO	75	Y=-26.736+11.026*SL	0.922	<0.0001
	MD	75	Y=-13.939+9.352*SL	0.801	<0.0001
Neuromast Width	SO	75	Y=-30.647+12.927*SL	0.833	<0.0001
	MD	75	Y=-15.264+10.984*SL	0.807	<0.0001

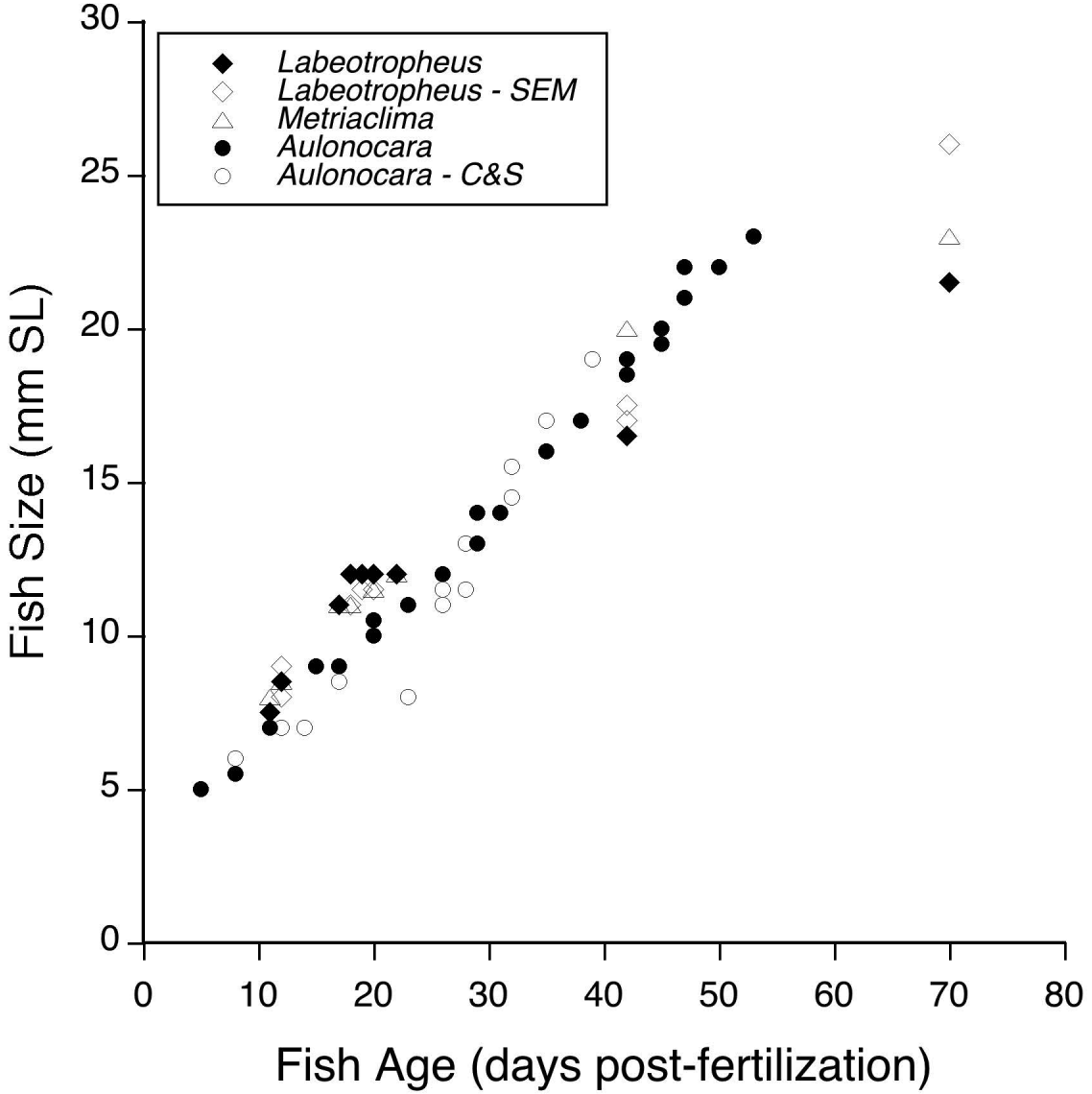

Webb et al., Figure 1

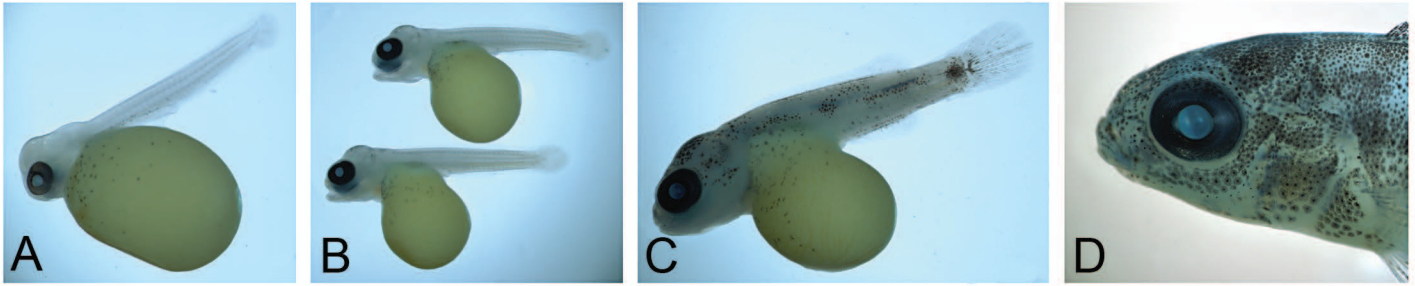

Webb et al., Figure 2.

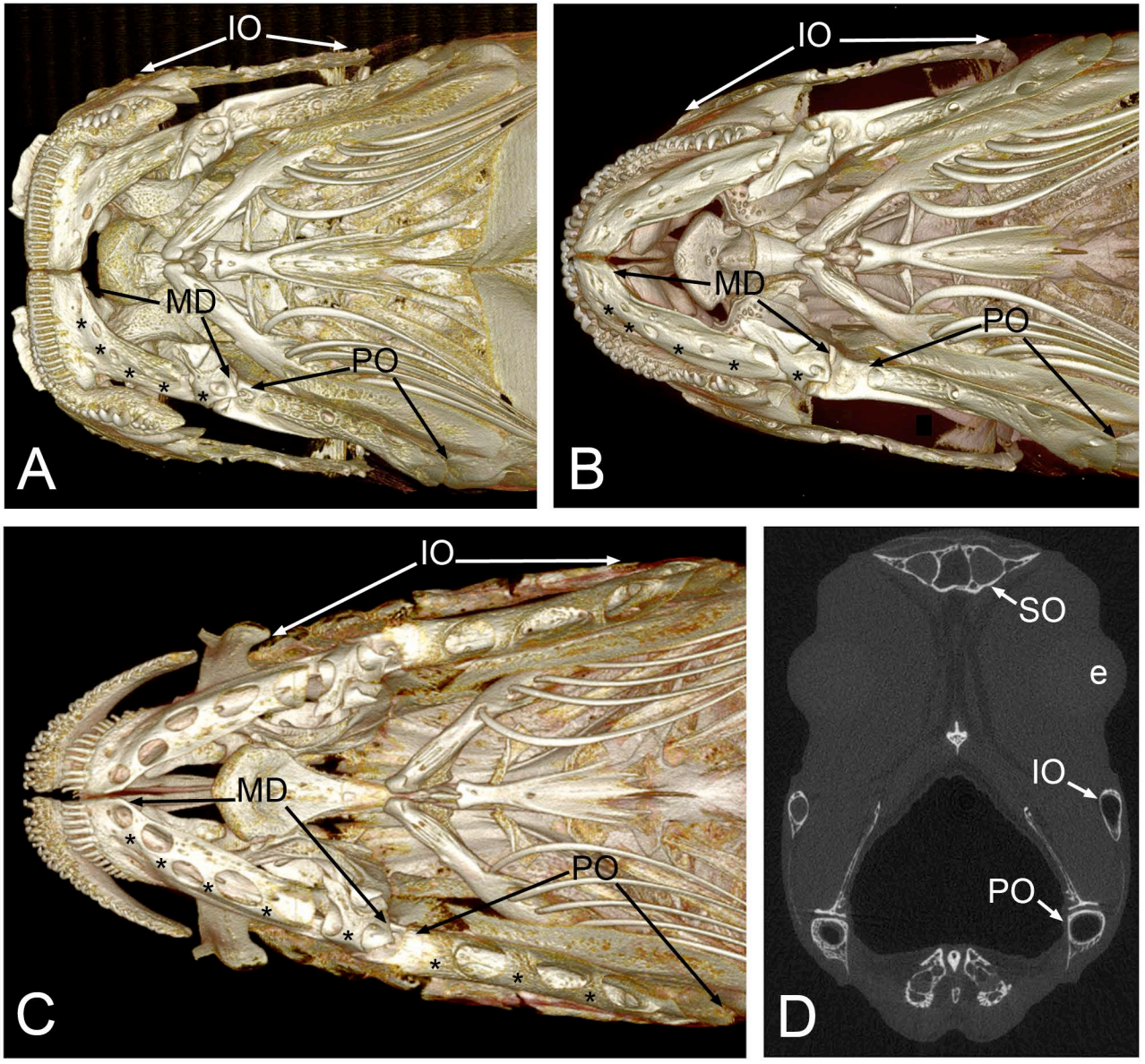

Webb et al., Figure 3

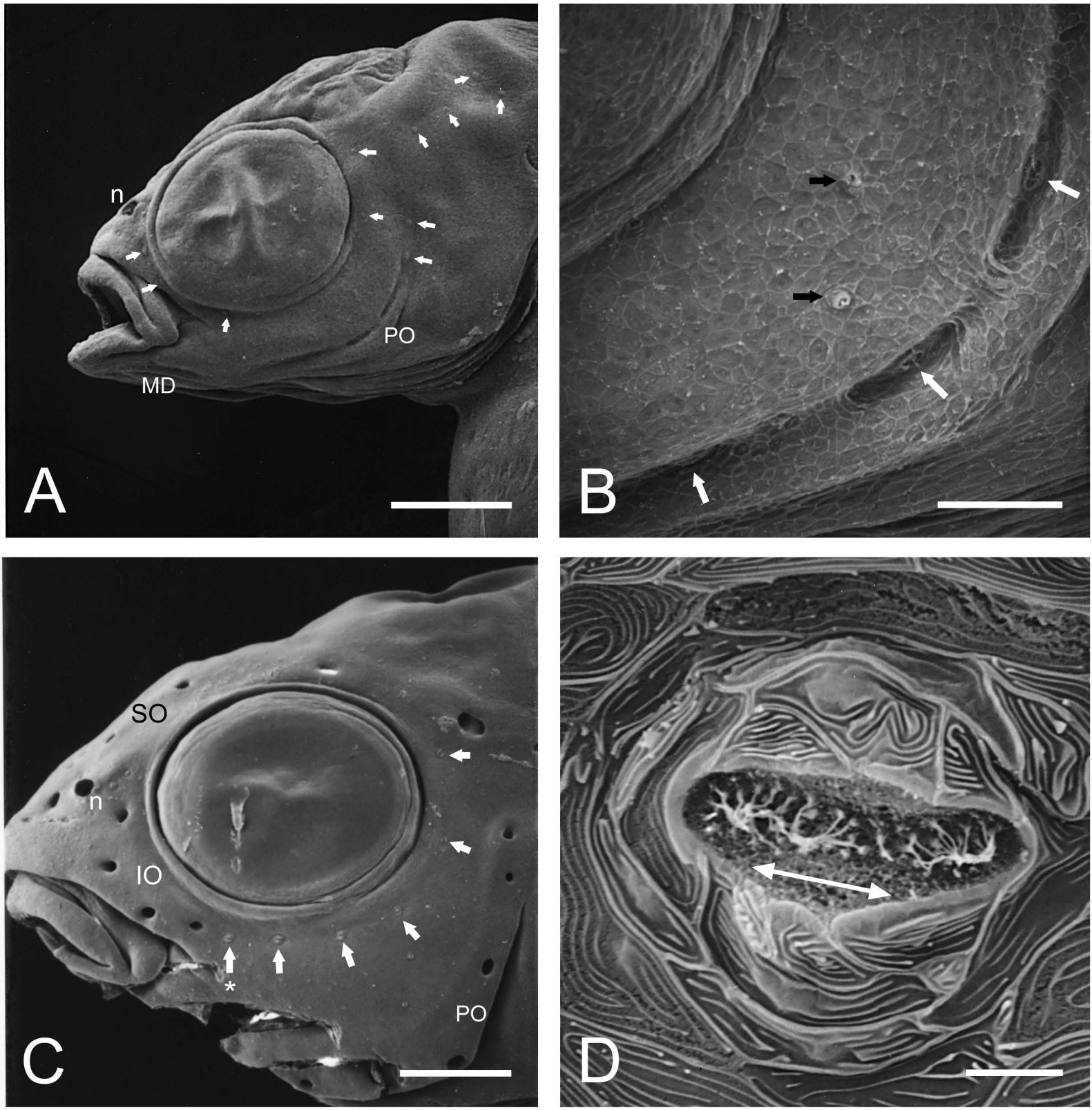

Webb et al., Figure 4

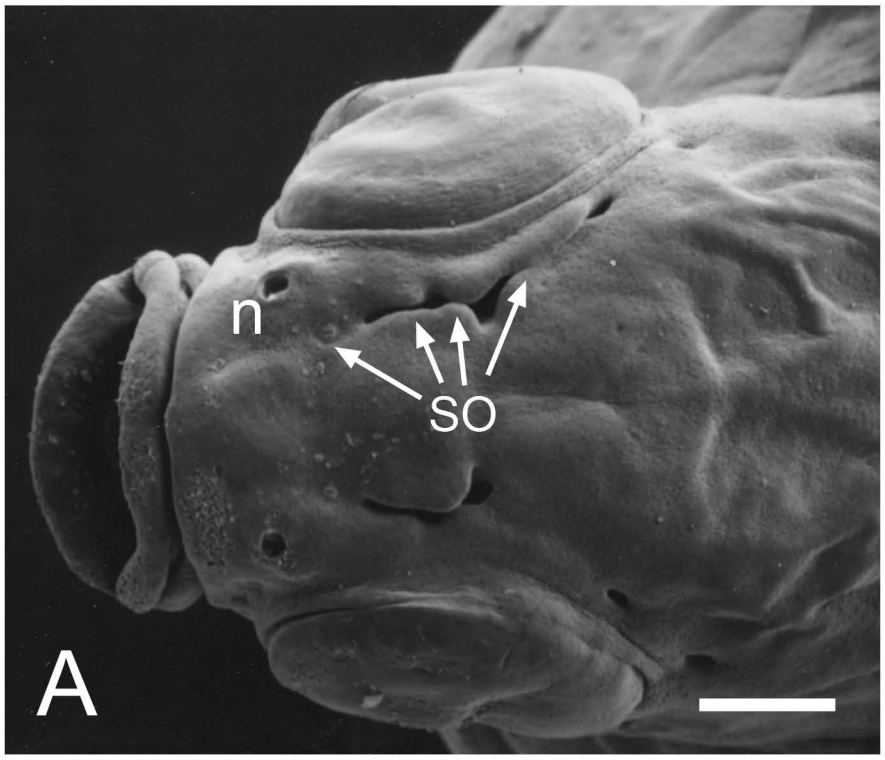
n
SO
A

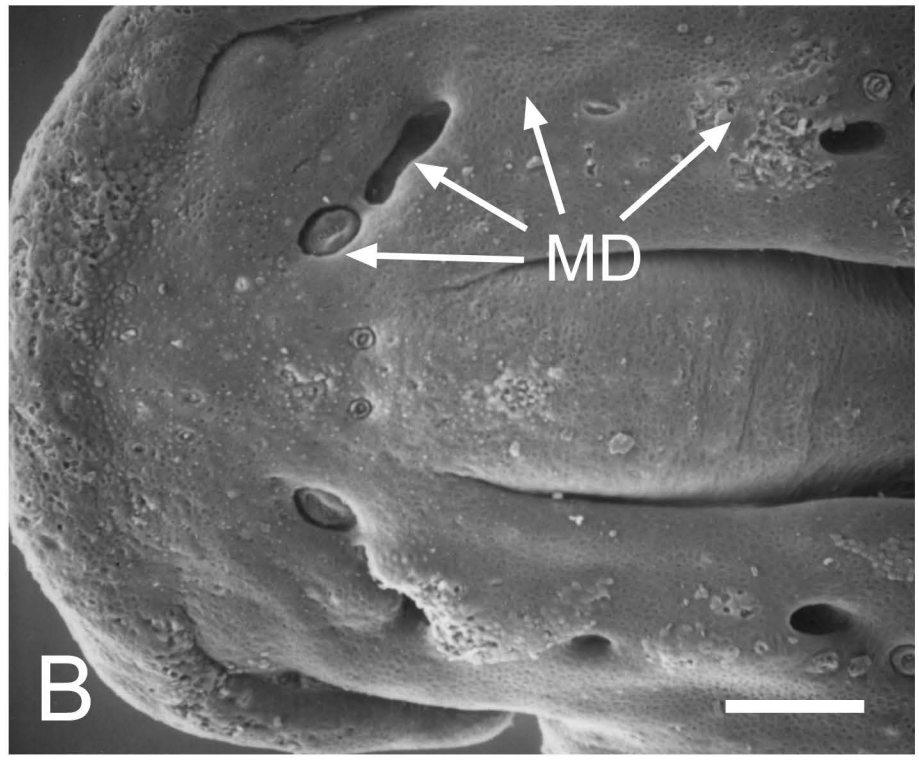
MD
B

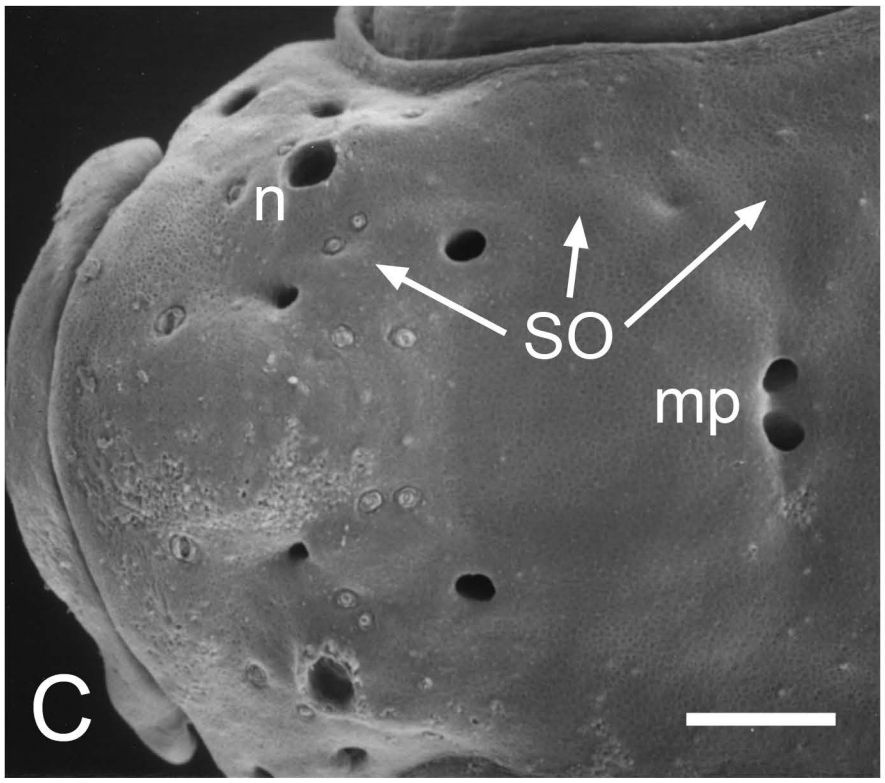
n
SO
mp
C

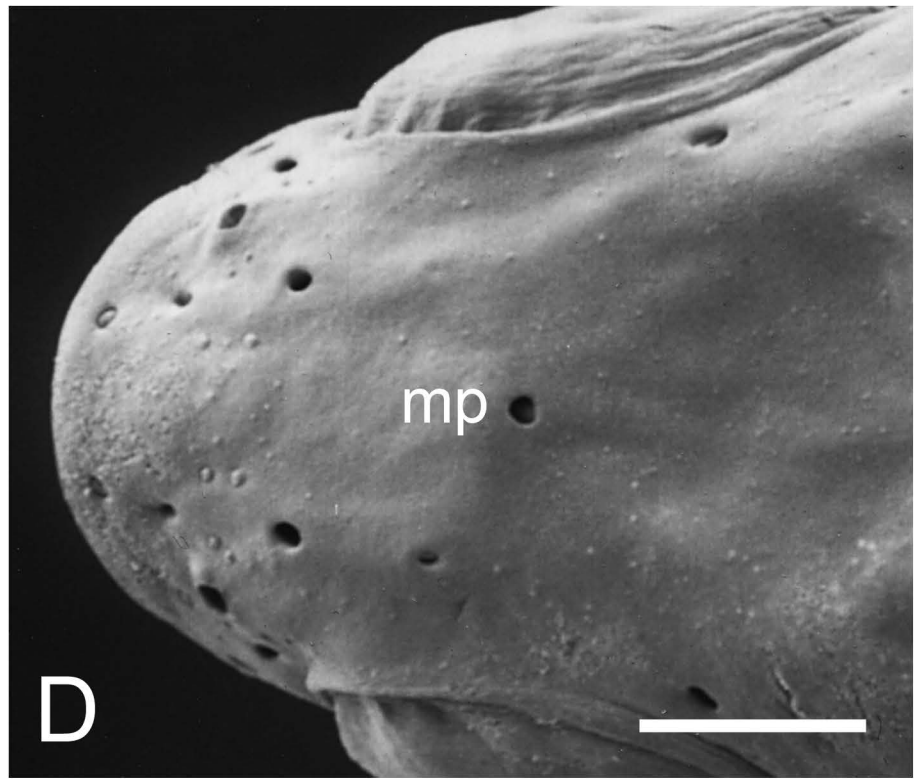
mp
D

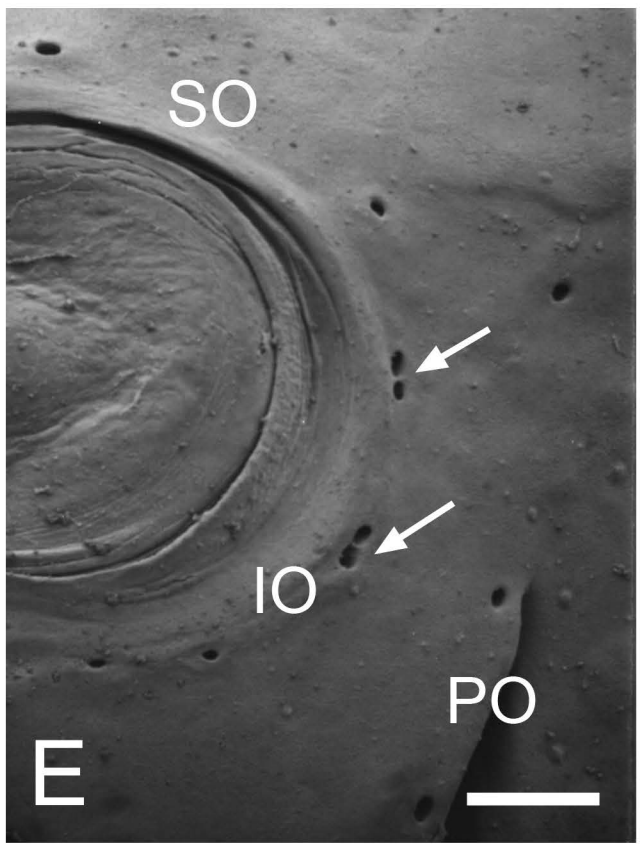
SO
IO
PO
E

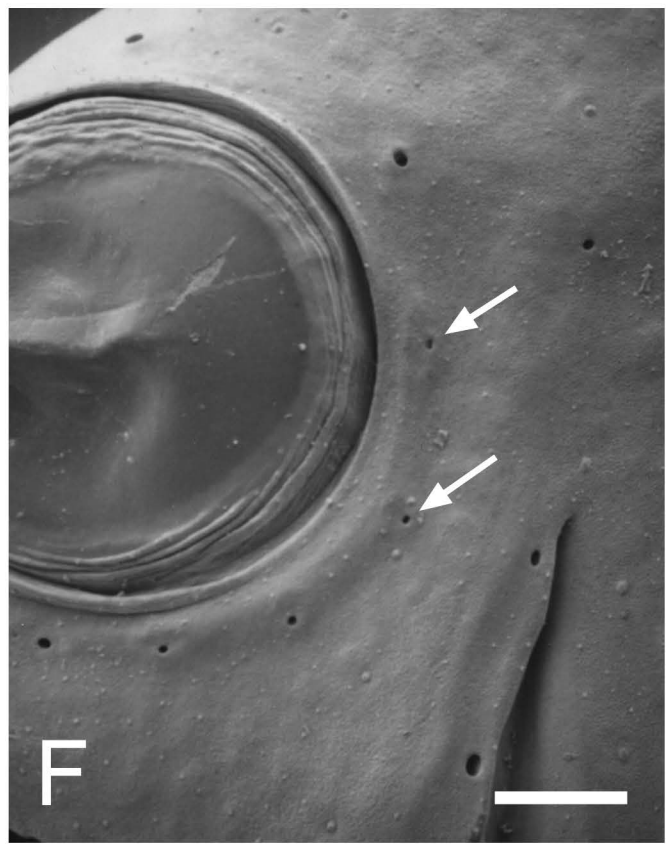
F

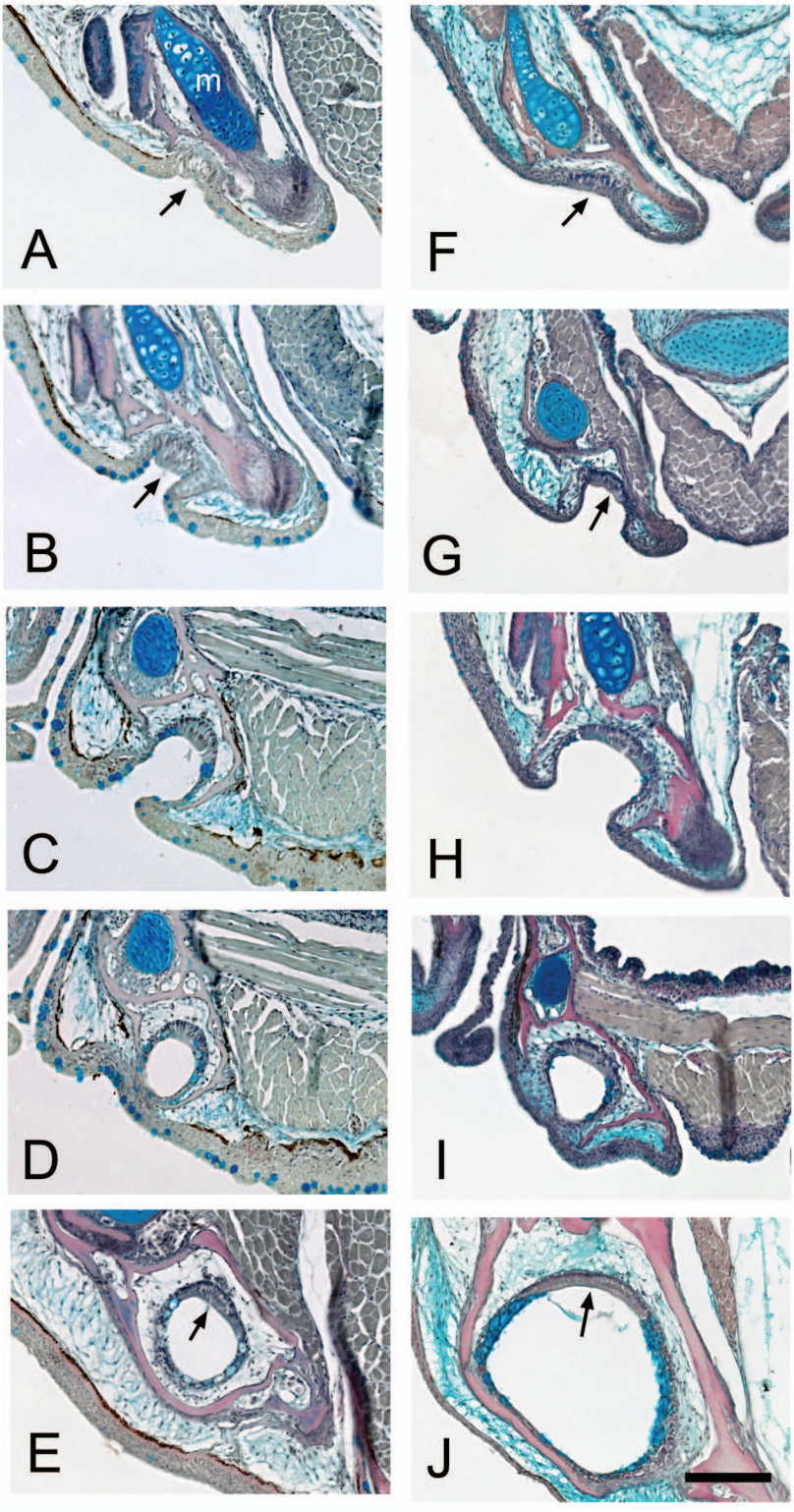

Webb et al., Figure 6

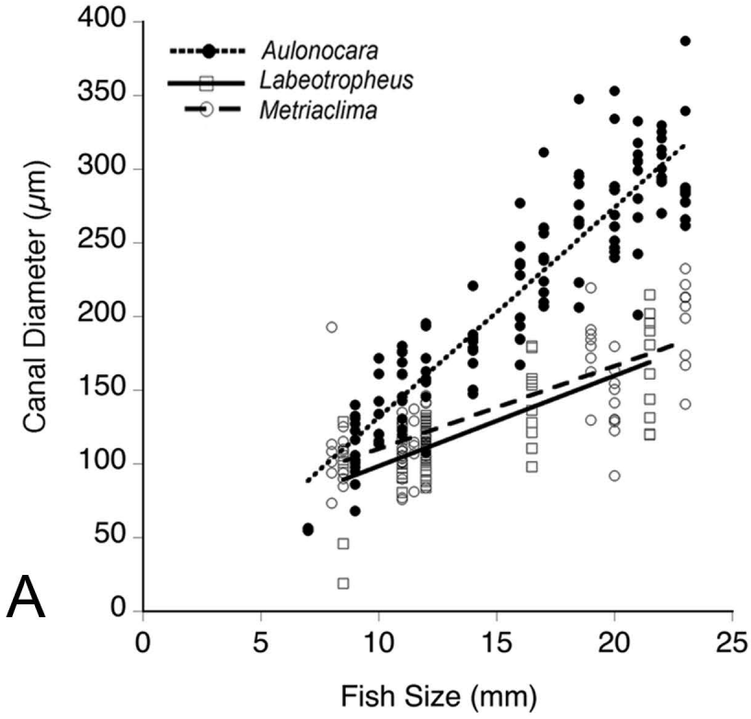

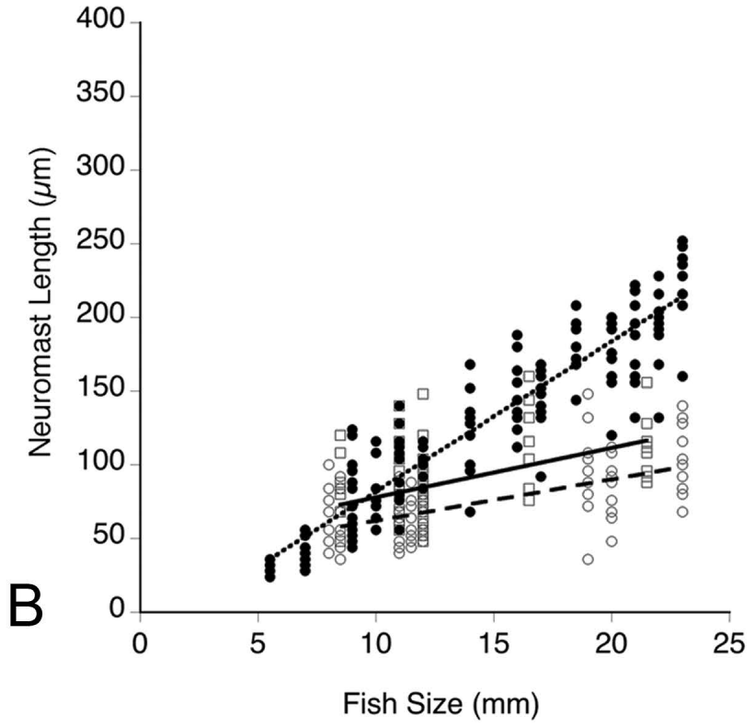

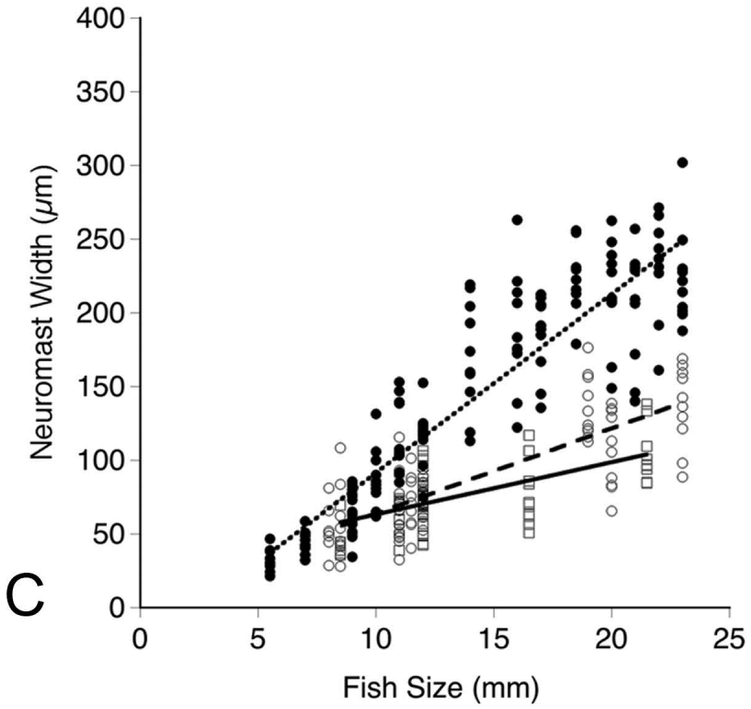

Webb et al., Figure 7